Supporting Information for

Self-Assembly and Nonlinear Optical Properties of N-Substituted Fulleropyrrolidine Bearing Adamantane

Yuhao Liu,[a,#] Kaipeng Zhuang,[a,#] Shuaishuai Liu,[b] Hongzhen Li,[b] Yiran Zhang,[a] Jinrui Li,[a] Nicolas Godbert,[c,] Hongguang Li[a,*]*

[a] Key Laboratory of Colloid and Interface Chemistry, Ministry of Education, School of Chemistry and Chemical Engineering, Shandong University, Jinan 250100, China.
[b] Key Laboratory and Technical Center in Shandong Yimeng Transportation Development Group Co., Ltd.
[c] MAT_INLAB (Laboratorio di Materiali Molecolari Inorganici), Centro di Eccelenza CEMIF.CAL, LASCAMM CR-INSTM della Calabria, Dipartimento di Chimica e Tecnologie Chimiche, Università della Calabria, 87036 Arcavacata di Rende (CS), Italy.

[*] Author to whom correspondence should be addressed, E-mail: *hgli@sdu.edu.cn*

nicolas.godbert@unical.it

[#] These authors contribute equally.

1. Sample preparation for evaluation of NLO properties

To perform NLO measurements, we doped microcrystals of Ad-C_{60} into PMMA matrix. The content of the microcrystals was kept at 1 wt%. In a typical experiment, 200 mg of PMMA was added to a solution containing 5 mL of a 2:3 mixture of CH_2Cl_2 and acetone. The mixture was homogenized using ultrasound for 10 min, after which time, an acetone dispersion of Ad-C_{60} microcrystals (2 mg/mL, 1 mL) was added. After being vortexed for 2 min and sonicated for 15 min, the mixture was immediately transferred to a quartz surface dish (60 mm in diameter) and stored at 25°C for 12 h. After evaporation of the solvent, the films were obtained.

The NLO properties of the composite films were evaluated using a Z-scan NLO spectrometer (model ZSQM-1) with a linearly polarized 5 ns laser at a wavelength of 532 nm, using the open aperture Z-scan technique. Details of the measurements and methods of data manipulation can be found in our previous work.[1-3]

2. Additional Scheme and Data

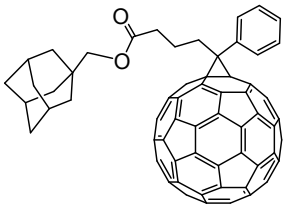

ACS Appl. Mater. Interfaces **2013**, *5*, 9579-9584
PCBM should be synthesized first

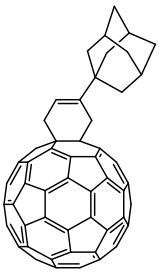

Nat. Commun. **2014**, *5*, 4877
Ad-containing oxetane is needed, during which dimethylsulfoxonium methylide will be used

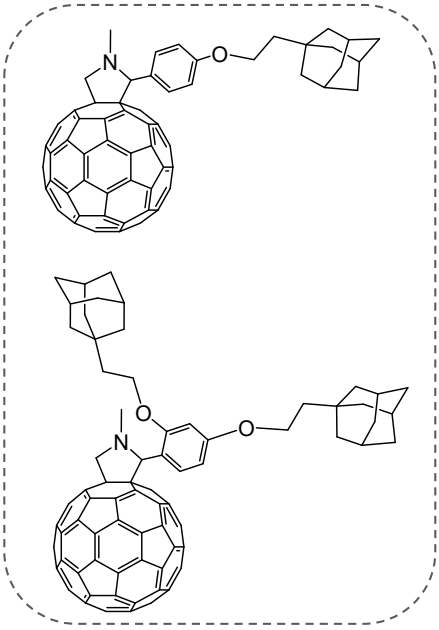

Nanoscale **2017**, *9*, 16375-16385
Ad-substituted benzaldehydes are needed

Scheme S1. Molecular structures of the Ad-C_{60} reported previously. Corresponding literatures and the key intermediates (not commercially available) needed for the preparation of the Ad-C_{60} are highlithted.

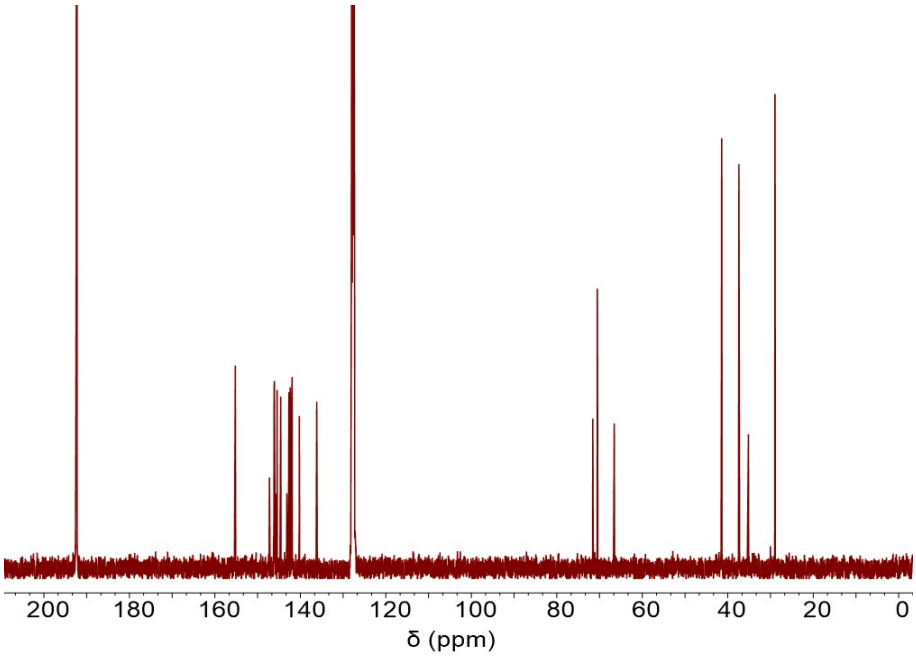

Fig. S1 ^{13}C NMR spectrum of the Ad-C_{60}.

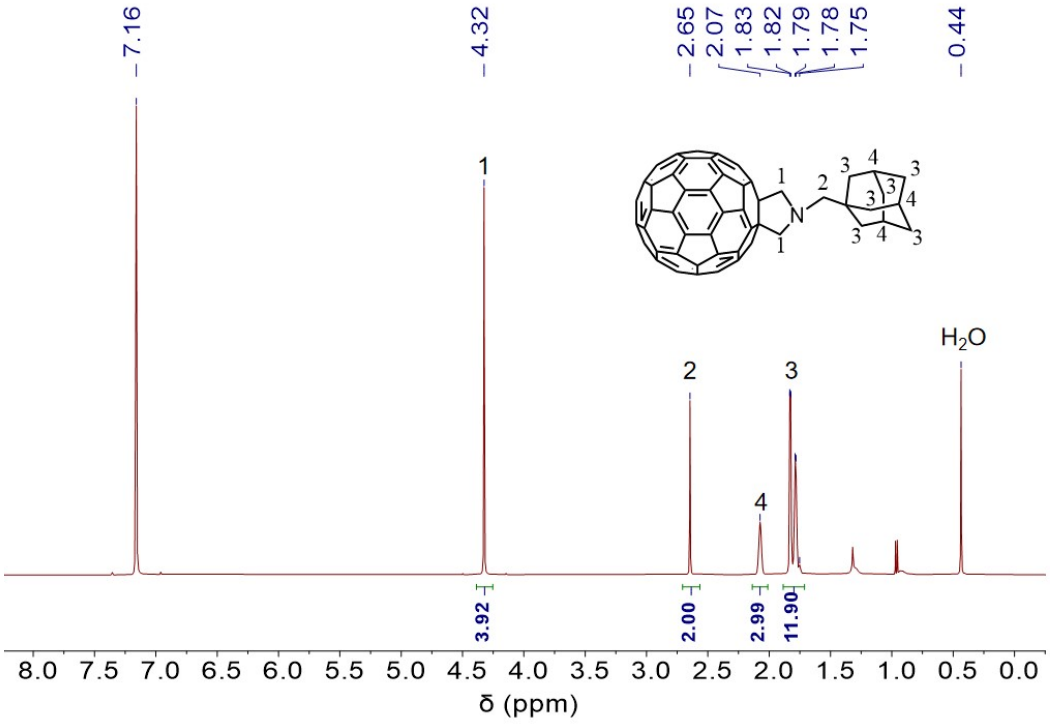

Fig. S2 ^{1}H NMR spectrum of the Ad-C_{60}.

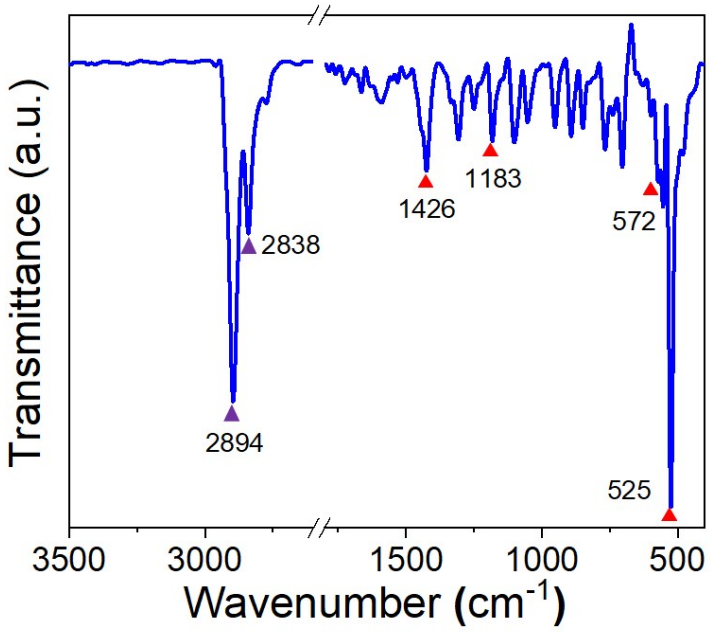

Fig. S3 FTIR spectrum of the Ad-C_{60}, with typical peaks marked (for detailed assignments, see discussion in the maintext).

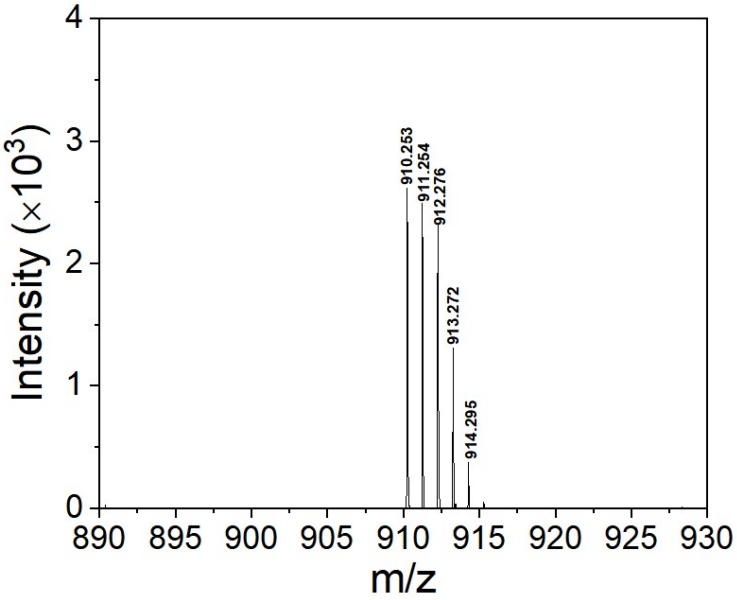

Fig. S4 MALDI-TOF-MS of the Ad-C_{60}.

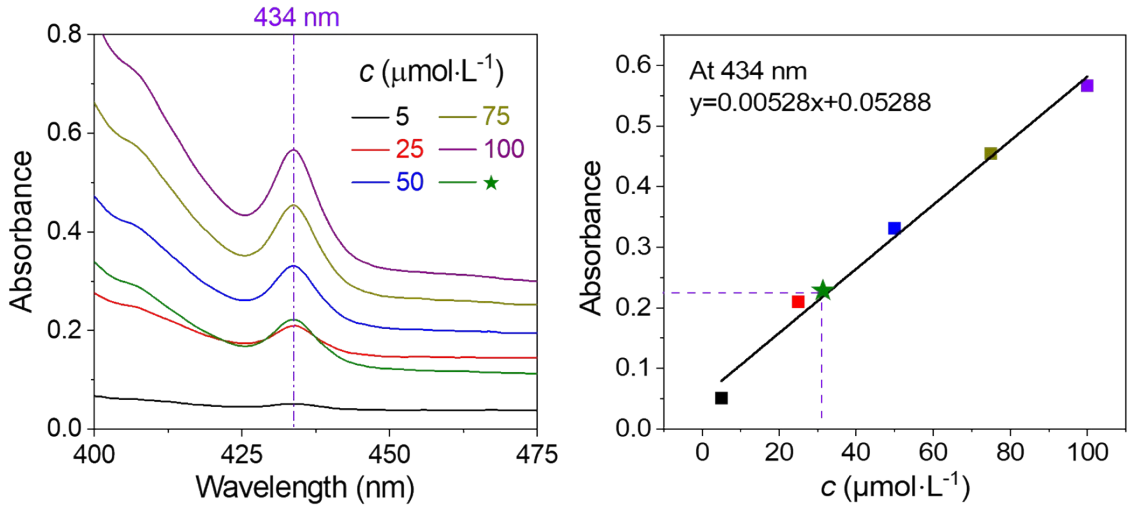

Fig. S5 An example showing the method to obtain the solubility of Ad-C_{60} in a given solvent. a) UV-vis absorption of Ad-C_{60} in *m*-xylene at varying concentrations as indicated. The curve marked by the star denotes the sample diluted 1000 times from the saturated solution. b) Linear fit of the data given in a. (Note: Solubilities in other solvents were obtained with the same method.)

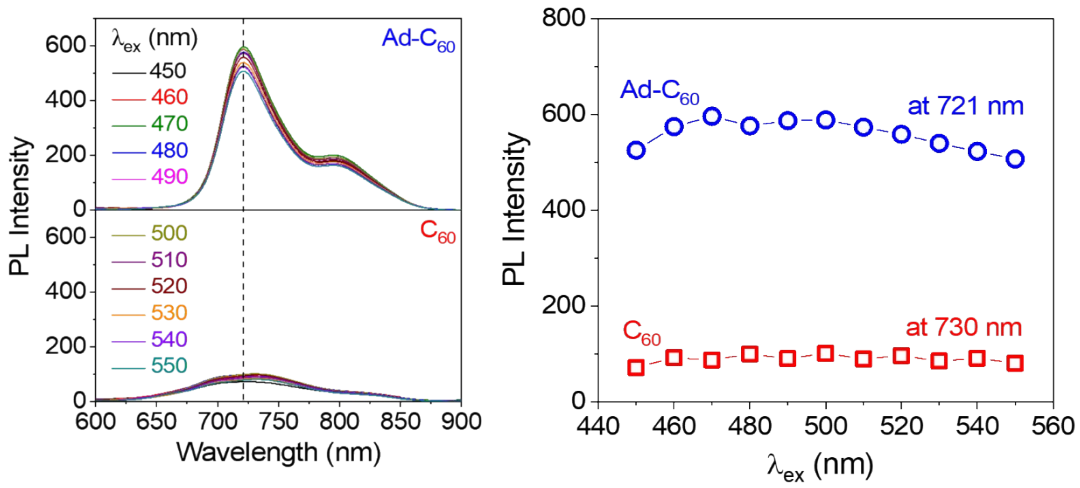

Fig. S6 a) Emission of Ad-C_{60} and unmodified C_{60} under different excitation wavelengths, recorded in *m*-xylene with a concentration of 1.0 mg·mL^{-1}. The dashed line is a guide for the eyes. b) Statistics of the PL intensity (at different emission wavelength for Ad-C_{60} and unmodified C_{60} as indicated) as a function of excitation wavelength for the data shown in a.

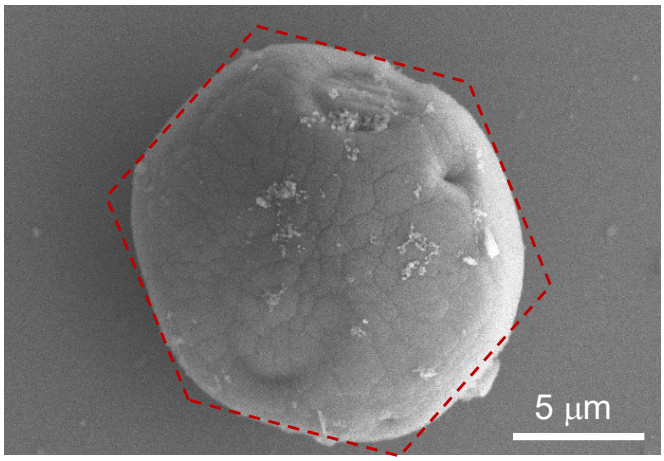

Fig. S7 SEM image of a typical crystal formed by Ad-C_{60} from *o*-xylene/IPA system. The condition of crystal preparation is the same with the sample given in Figure 2a, b in the maintext. The dashed hexagon is a guide for the eyes.

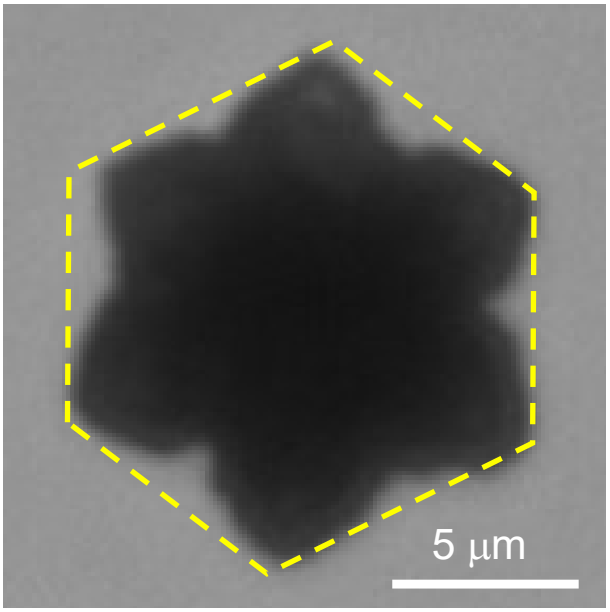

Fig. S8 TEM image of a typical crystal formed by Ad-C_{60} from *o*-xylene/EtOH system. The condition of crystal preparation is the same with the sample given in Figure 2c, d in the maintext. The dashed hexagon is a guide for the eyes.

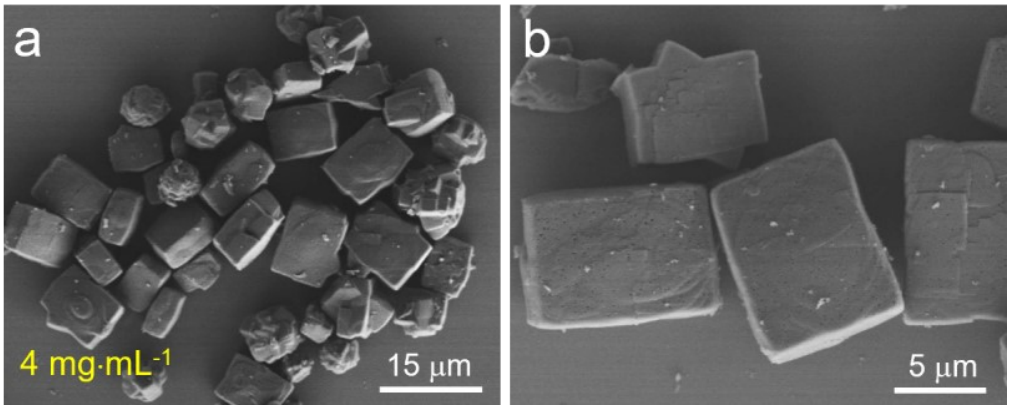

Fig. S9 a) A typical SEM image of the crystals formed by Ad-C_{60} from m-xylene/EtOH with a volume ratio of good solvent to poor solvent of 1:7. The concentration of Ad-C_{60} is 4 mg·mL^{-1}. b) A magnified image highlighting the morphology of the bricks.

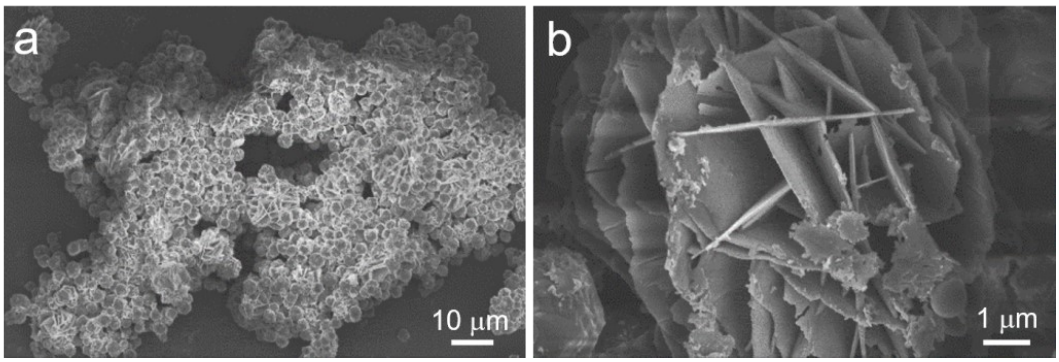

Fig. S10 a) A typical SEM image of the crystals formed by Ad-C_{60} from *p*-xylene/EtOH with a volume ratio of good solvent to poor solvent of 1:10. The concentration of Ad-C_{60} is 3 mg·mL^{-1}. b) A magnified image highlighting the morphology of the desert-rose like crystals.

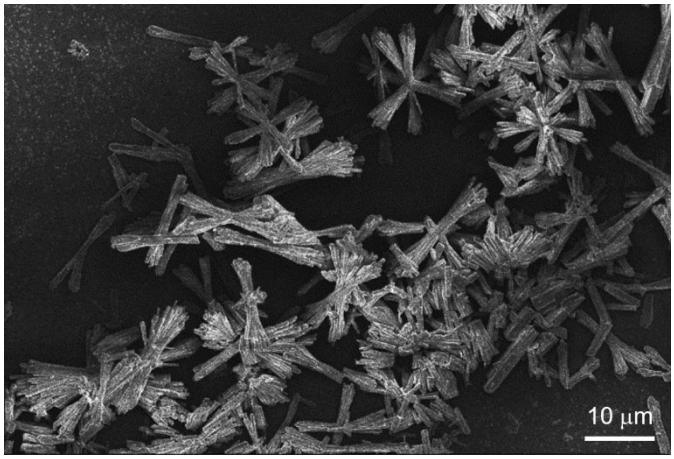

Fig. S11 a) A typical SEM image of the crystals formed by Ad-C_{60} from CCl_4/TBA with a volume ratio of good solvent to poor solvent of 1:10, taken with a lower magnification compared to that given in the maintext (Figure 2k). The concentration of Ad-C_{60} is 4 mg·mL^{-1}.

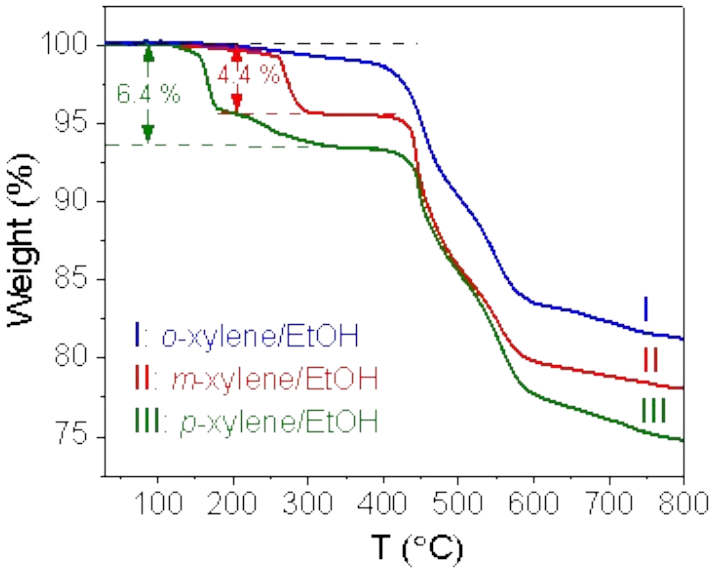

Fig. S12 TGA curves of the superstructures formed by Ad-C_{60} crystals in xylene/EtOH systems.

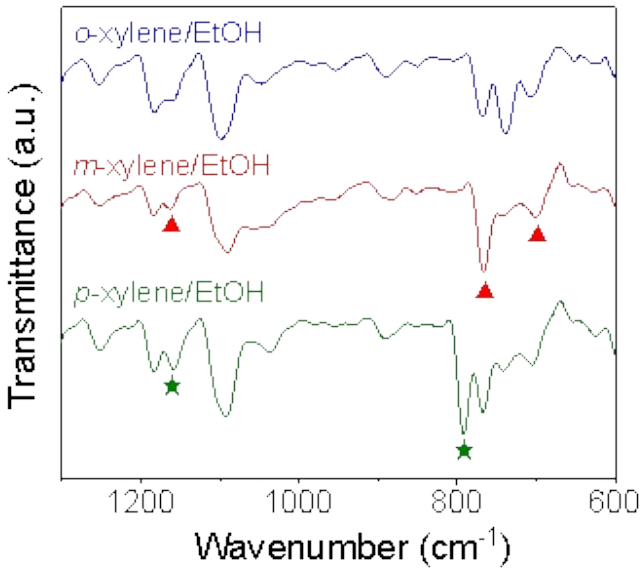

Fig. S13 FTIR spectra of the superstructures formed by Ad-C_{60} crystals in xylene/EtOH systems.

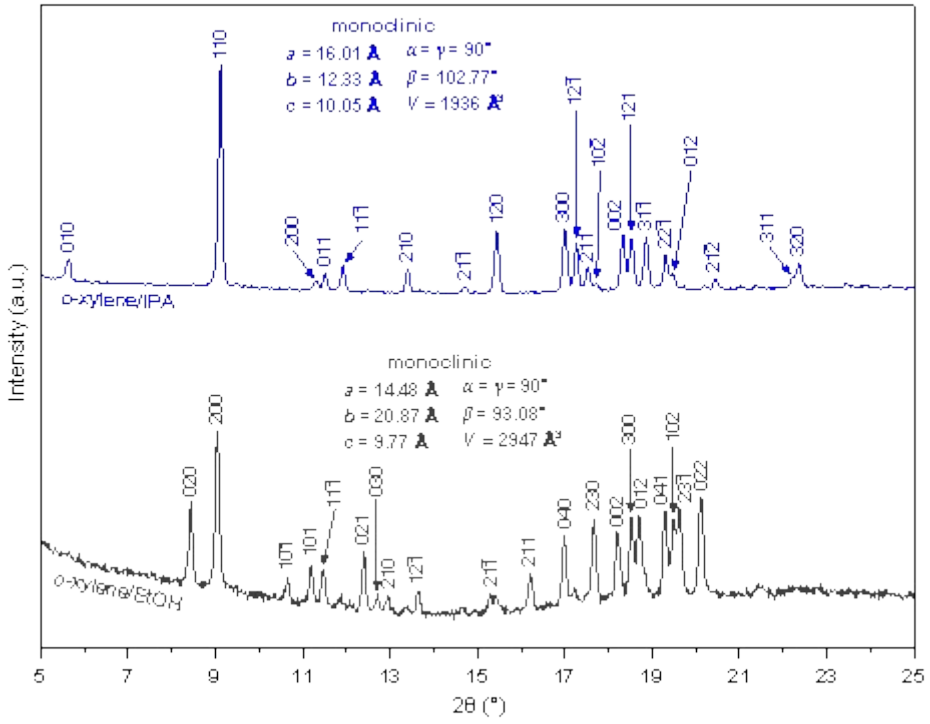

Fig. S14 XRD pattern of the superstructures formed by Ad-C_{60} crystals in *o*-xylene/EtOH, in comparison with that formed in *o*-xylene/IPA (already given in the maintext). The type of the lattice with detailed parameters are included inset.

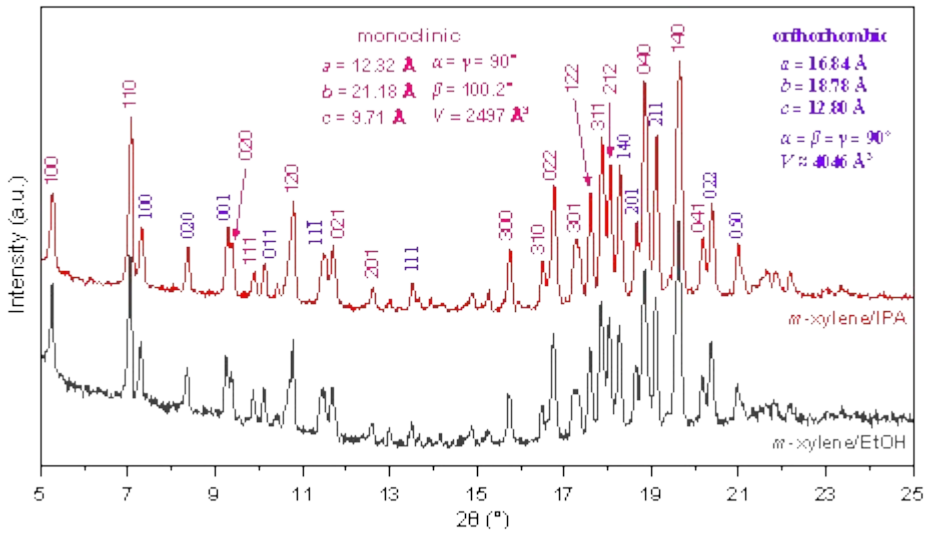

Fig. S15 XRD pattern of the superstructures formed by Ad-C_{60} crystals in *m*-xylene/EtOH, which is the same with that formed in *m*-xylene/IPA (already given in the maintext).

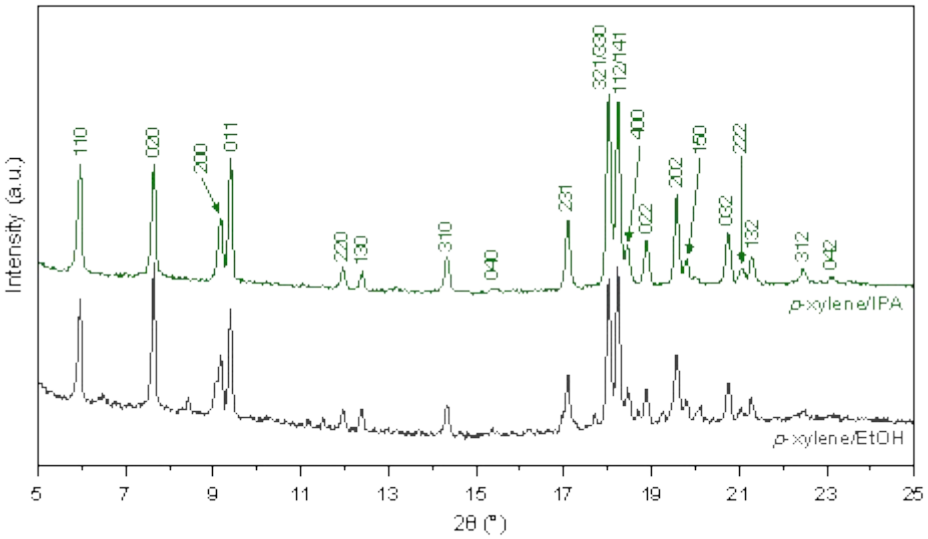

Fig. S16 XRD pattern of the superstructures formed by Ad-C_{60} crystals in *p*-xylene/EtOH, which is the same with that formed in *p*-xylene/IPA (already given in the maintext).

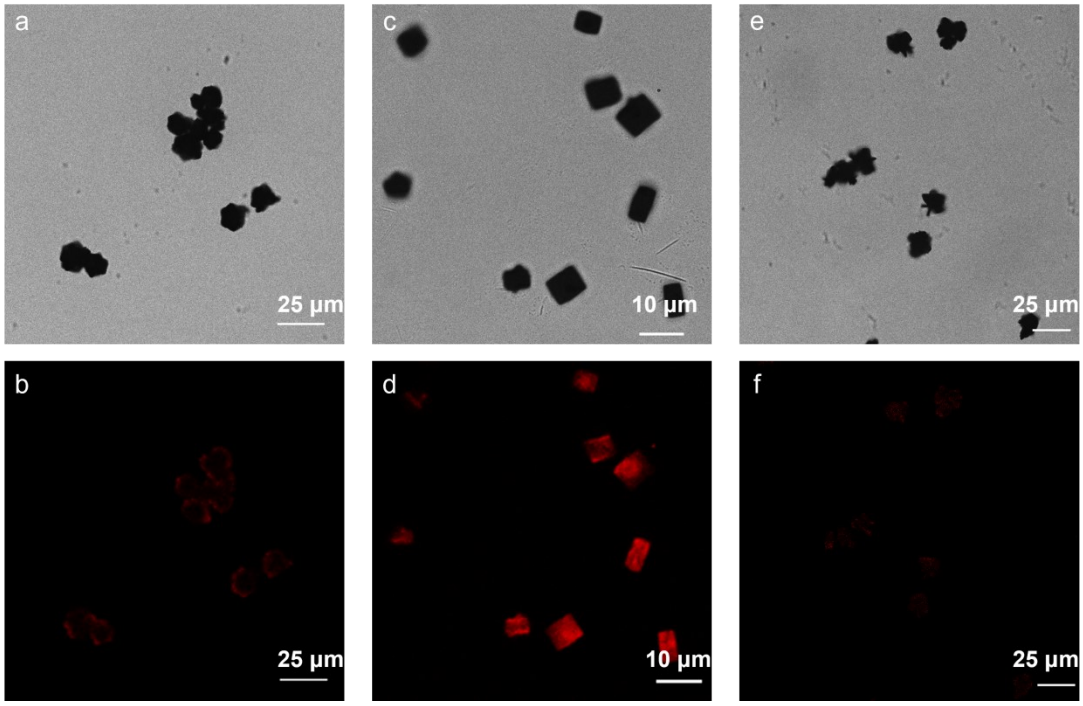

Fig. S17 Confocal fluorescence microscopic images in bright (the top row) and fluorescent channel (the bottom row), respectively, of the superstructures engineered from *o*-xylene/IPA (a, b), *m*-xylene/IPA (c, d) and *p*-xylene/IPA (e, f).

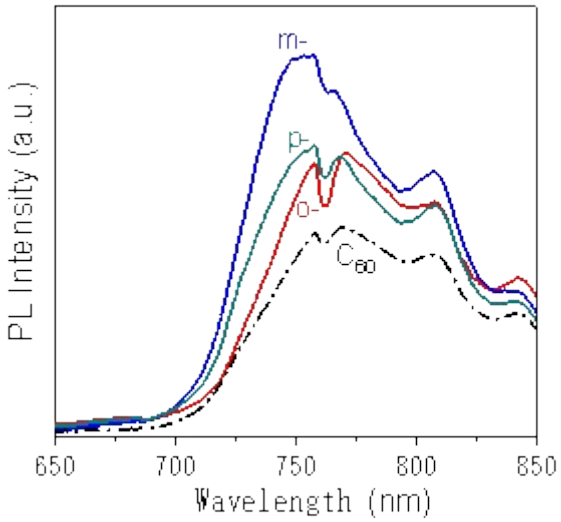

Fig. S18 Microfluorescence spectra of three crystals engineered from xylene/EtOH systems. For comparison, the curve from as-synthesized Ad-C_{60} powder is also given.

References

1. J. Li, H. Li, J. Hao, Fullerene superlattices containing charge transfer complexes for an improved nonlinear optical performance. *Nanoscale*, **2022**, *14*, 2344–2351.

2. J. Li, Y. Bi, Z. Liu, Z. Yang, X. Xin, L. Feng, H. Li, .J. Hao, Chiral metal nanocluster within nanoarchitecture of fullerene C_{60}: Chirality transfer and improvement of nonlinear optical property. *Nano Res.*, **2024**, *17*, 9255-9260.

3. J. Li, H. Xie, D. Sun, H. Li, X. Xin, Co-assemblies of Silver Nanoclusters and Fullerenols With Enhanced Third-Order Nonlinear Optical Response. *Small Methods*, **2025**, 2401782.